

Series production data calibration

by *pmdtechnologies*

Abstract

The purpose of this document is to summarize the calibration procedure of 3D time-of-flight cameras respecting series production constraints. The primary aims of this procedure are its capability of full automation, fail safety, reproducibility and its respect of timing constraints

Table of Contents

Abstract.....	1
Table of Contents	1
List of Figures.....	2
List of Tables	2
1. Introduction.....	3
2. Hardware Set-Up.....	5
2.1. Box 1 – Optical Model, FPN, FPPN.....	6
2.2. Box 2 – Wiggling	7
3. Software Set-Up / Algorithms.....	9
3.1. Intrinsic Lens Calibration	9
3.1.1. Calibration Model	9
3.1.2. Feature Acquisition and Evaluation	10
3.1.3. Quality Metric	11
3.1.4. Global Lens Calibration	11
3.2. Wiggling	12
3.2.1. Quality Metric	15
3.3. Offset and FPPN Correction.....	15
3.4. Mutual Dependency of Wiggling and FPPN	16
3.5. Temperature Drift.....	16
3.6. Illumination Mask	17
4. Data processing.....	18
5. Calibration Results.....	19
5.1. Comparison of the Individual Steps.....	19
5.2. Metric-Based Comparison.....	22
6. Parameters.....	23
References.....	23
Document History.....	24

List of Figures

Figure 1: Symbolic box depiction	3
Figure 2: Calibration flow diagram	4
Figure 3: Undistortion after lens calibration.....	4
Figure 4: FPPN.....	4
Figure 5: Wiggling (symbolic)	5
Figure 6: Pattern for the Optical Model (left: model, right: photo of a prototype)	6
Figure 7: Common calibration box for FPPN and lens by usage of LEDs	6
Figure 8: Wiggling Box Prototype	7
Figure 9: Diffusion layer between fibre end and detector	8
Figure 10: Intrinsic lens parameters without distortion	10
Figure 11: Feature point detection for the lens calibration	11
Figure 12: Fiber Segmentation (left: spot detection; right: ordered blobs)	12
Figure 13: Fiber segmentation.....	13
Figure 14: Phase Wiggling (the numbers denote the individual fibers).....	13
Figure 15: Amplitude Wiggling.....	14
Figure 16: Distance deviation caused by thermal drift – linear relationship	16
Figure 17: Temperature drift	17
Figure 18: Illumination Mask Example	17
Figure 19: Data Processing Part 1/2 (blue parts require calibration inputs).....	18
Figure 20: Data Processing Part 2/2 (blue parts require calibration inputs).....	18
Figure 21: Opposed Calibration Inclination Angles	19
Figure 22: Phase Wiggling Compensation with prototype and series calibration.....	20
Figure 23: One Row of the FPPN	21
Figure 24: Difference to Ground-Truth with Applied Calibration; reference pixel in the middle	22

List of Tables

Table 1: Calibration Steps Overview (*additional computational time depends on CPU processing power)	3
Table 2: Hardware Set-Up Deliverables	5
Table 3: Fiber Types - Advantages and Drawbacks	9
Table 4: Set-up Parameters.....	23

1. Introduction

All calibration steps can be performed by placing the camera module subsequently into two different calibration boxes. These boxes are described in the second chapter, and the calibration algorithms are described in the third chapter. For a general idea of the calibration concept, have a look at the video [2] showing a two-box set-up and the calibration flow. Table 1 and Figure 1 show the different systematic sources of error which need to be calibrated and a symbolic depiction of the recommended set-up for series-production calibration purposes. This recommended set-up will be detailed in the following chapter.

Step	Concept	Order of Error	Measurement Time Effort*	Box
FPN, FPPN	adequate number of frames for averaging of a well-positioned plane wall ^(1a)	8cm	2.5s	1
Wiggling	adequate number of frames for averaging @ different distances of well-defined time of flights using fibers to simulate different distances ⁽²⁾	8cm	2.5s	2
Lens Calibration	single shot image of a well-positioned pattern ^(1b)	-	1s	1
Thermal Drift	Distance deviation is a linear function of the temperature difference; determined globally	6cm	-	-

Table 1: Calibration Steps Overview (*additional computational time depends on CPU processing power)

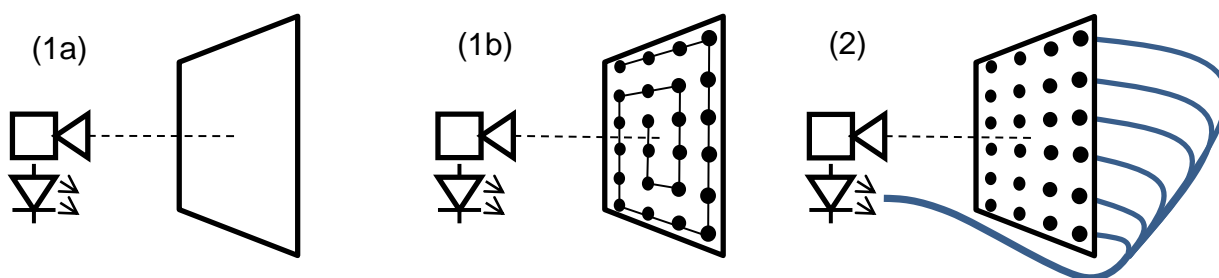


Figure 1: Symbolic box depiction

Figure 2 shows the sequence, in which the individual steps are performed. This sequence is not arbitrary.

- **Intrinsic Lens calibration:** The phase and distance calculation of each pixel in a pmd sensor delivers the radial component of an object in a spherical coordinate system. In order to transform this information to the more practical Cartesian xyz-three-dimensional position for each pixel, we need to know the individual direction each pixel is looking at. This direction is given by the lens system of the camera. The described calibration method requires only the 2D amplitude data and is independent from phase accuracy and other calibration steps. Since intrinsic lens calibration is not only a pmd typical calibration step and 2D cameras are also affected by lens distortion, there are several well-known methods provided for example by OpenCV [5]. The calibration models radial and tangential distortion so that the application of the calibration to the images makes lines, which are physically straight, also straight in the projection; cf. the example in Figure 3.

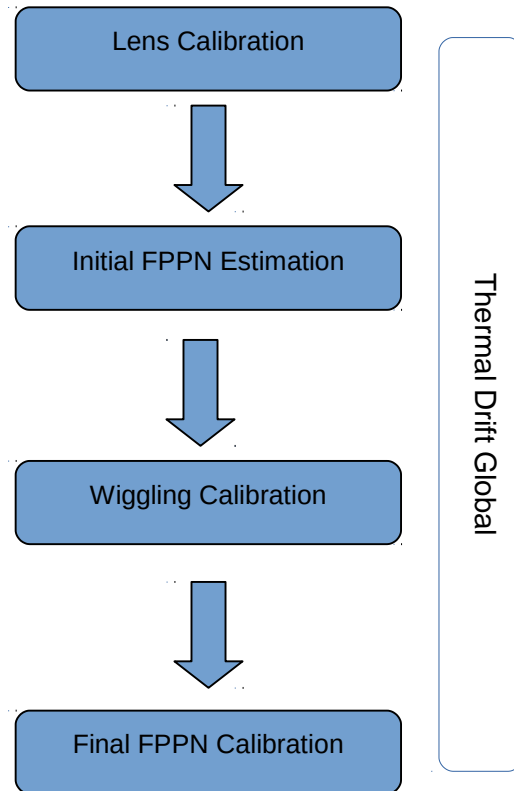


Figure 2: Calibration flow diagram

- **FPN and FPPN:** The signal shapes and the initial phase delay between emitted light and pmd pixel modulation are influenced by various system parameters. Depending on the required absolute accuracy, each pixel value needs to be corrected by a pixel and sensor individual offset level. There is a fixed pattern of intensity offsets (fixed pattern noise, FPN) and a different fixed pattern of distance offsets (fixed pattern phase noise, FPPN). The FPPN is estimated initially with data including wiggling effects. Figure 4 shows an example image of the FPPN.

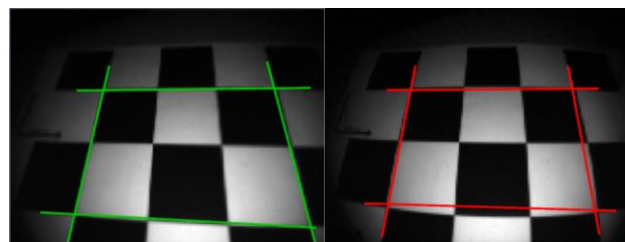


Figure 3: Undistortion after lens calibration

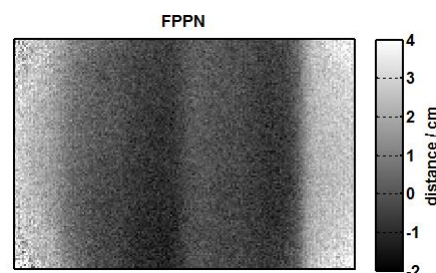


Figure 4: FPPN

- **Wiggling:** As the straightforward phase calculation based on trigonometric interpolation on four samples of the correlation function neglects the real signal shape, i.e. higher-order frequency parts of the correlation signals, a systematic deviation arises, which is a function of the measured phase. See Figure 5 to get an idea of the wiggling effect.
- **Final FPPN Calibration:** After computing the wiggling compensation parameters, the FPPN can be derived using the same images as before but with compensated wiggling effect.
- **Temperature drift:** Some modulation signal generation parts are temperature sensitive. This leads to a temperature dependent signal delay, so that the measured phase changes with temperature. This delay is corrected by measuring the temperature with an internal sensor and correcting the drift by an adequate approximation of the deviation – typically, a linear approximation is optimal. The calibration parameters are determined globally as they are fix for a given design and they do not need to be calibrated for each camera. In order to be ensure that these global parameters are still applicable, random samples can be picked to check the parameters either using self-heating or by means of an external heating ('climate chamber').

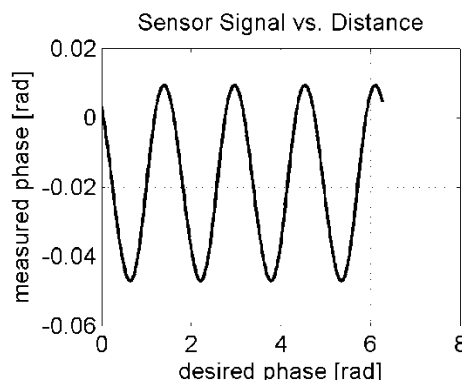


Figure 5: Wiggling (symbolic)

2. Hardware Set-Up

The hardware set-up needs to provide the information listed in Table 2 to the individual calibration steps.

Calibration Step	Set-Up Deliverables
Optical Model	Defined pattern of clearly discernible feature points covering the whole FOV
FPN and FPPN	Homogeneous planar pattern covering the whole FOV
Wiggling	Sampling points with ground-truth phase values distributed over the unambiguous range for as few different pixels as possible

Table 2: Hardware Set-Up Deliverables

These requirements can be met by designing two different boxes for the calibration, one for the FPPN, FPN and lens calibration and a second one for the wiggling calibration. When using identical mechanical dimensions for these boxes, they can share one common lid to which the camera module is fixed so that the transition from one box to the other is fail-safe and fast. The following two sections describe these two proposed boxes in detail. Each section summarizes the crucial aspects to keep in mind when thinking about variations or optimizations of this set-up.

2.1. Box 1 – Optical Model, FPN, FPPN

The relationship between the world and pixel coordinates can be derived by analyzing intensity images of a well-known pattern. **pmd** proposes a CNC-manufactured flat aluminum plate with a regular grid of small drilling holes with precisely known world coordinates. These holes shall contain switchable NIR LEDs. The pattern can be seen in Figure 6.

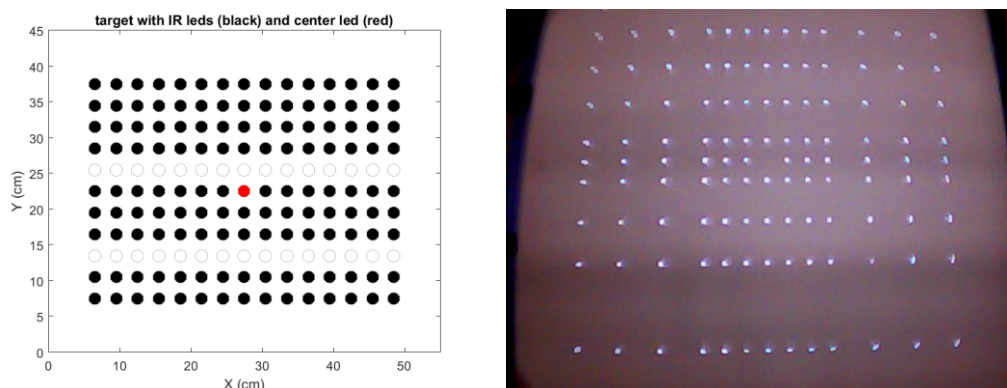


Figure 6: Pattern for the Optical Model (left: model, right: photo of a prototype)

In general, such a pattern needs to meet the following requirements:

- Discernibility: the sampling points need to be clearly discernible
- Appropriate dimensions: the size must be chosen in way that the pattern is projected to a sufficient number of pixels at the chosen focusing distance while the total number of sampling points is maximized at the same time. The pattern should fill the complete FOV.
- *If using a printed pattern instead of the switchable LEDs:* Feature clarity: the distinct feature of the pattern needs to be detected reproducibly and precisely. The feature points in the 3D space can be derived from squares: the edge points are detected, the diagonals are computed and then the points of intersection are the feature points used subsequently. The mid points of circles can also be used, if the fact, that mid points do not necessarily match the mid points of ellipses when transformed projectively, is not considered to be relevant [4, p. 343].

For the FPPN and the FPN correction, a homogeneous non-specular target is required, which covers the whole FOV. Avoid ambient light influences, stray light and multi-path propagation, i.e. it is advisable to place the target in a closed housing where those areas, which are not part of the field of view, are covered with a highly absorbingly material such as EPDM.

The reason why both FPN/FPPN and the optical model set-ups can be combined in one box is that a number of LEDs can be used to shine through a homogeneous non-specular target and thus illuminate the circular points required for the optical model feature acquisition – see Figure 7.

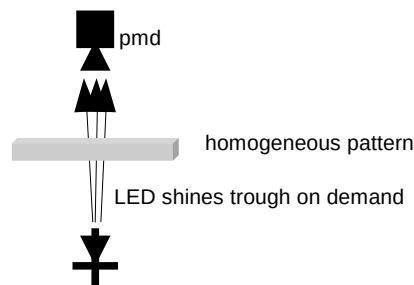


Figure 7: Common calibration box for FPPN and lens by usage of LEDs

In general, it is also possible to use a printed pattern for the lens calibration if a separate target is provided for the FPN and FPPN calibration (i.e. if there is one additional calibration box). However, this is not recommended by **pmd**.

2.2. Box 2 – Wiggling

As described above, the wiggling is a systematic function of the measured phase. In order to measure this effect, an adequate number of sampling points of the deviation between the true and the measured phase is required. So, the hardware set-up needs to provide points with different real phases. This can be achieved in several ways: the distance between a fix target and the camera can be varied or a scene with different distances spread over the image can be used. For a fast calibration with a simple single-shot set-up, the latter approach is more suitable, and the different distances can also be achieved by delaying the phase of light emitting points in the image, e.g. by using fibers with different lengths.

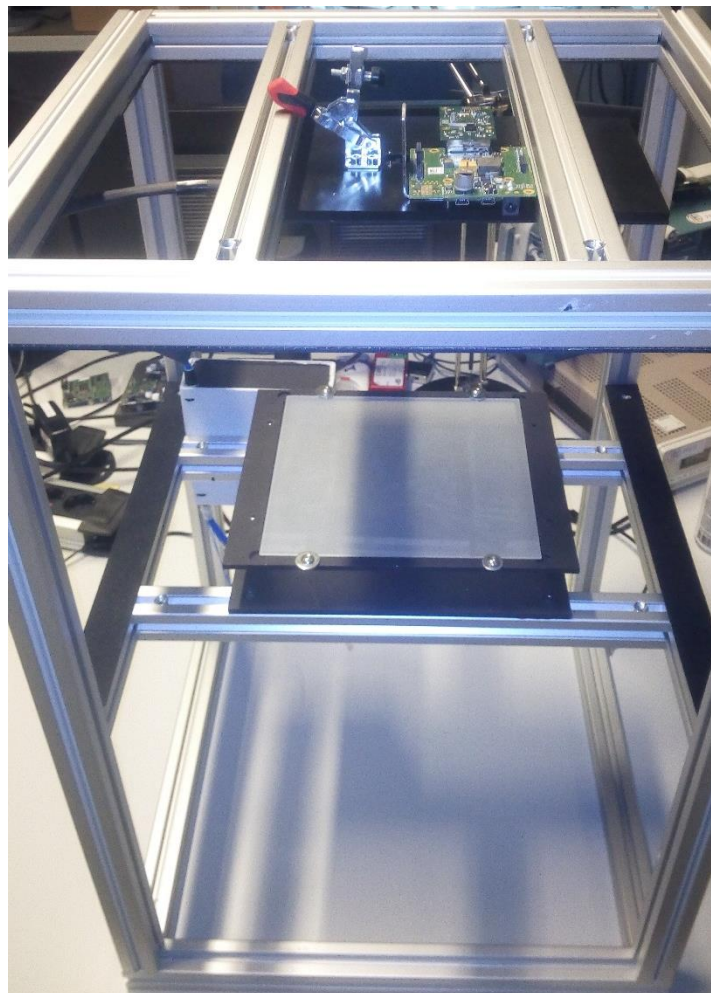


Figure 8: Wiggling Box Prototype

The prototype – see Figure 8 – consists of number of fibers with different lengths which redirect the modulated light emitted by the VCSEL so that the other end of the fiber points to the camera. In order to spread the phase information over more than only a part of a pixel, an optical diffusion layer is mounted on a plane in between. This is shown in Figure 9.

The data evaluation algorithm (cf. section 3.2) needs to know the expected phase value of the individual fibers. The determination of the expected values by measuring the total length of the fibers including the coupling distance has proven to be difficult due to the unknown propagation inside the fibers. This is why a one-time calibration of the fiber lengths by means of a golden sample is required, i.e. a device, which was calibrated using a linear translation stage and which is equivalent to the devices being calibrated subsequently, indicates fiber lengths after applying the reference calibration to the measurement.

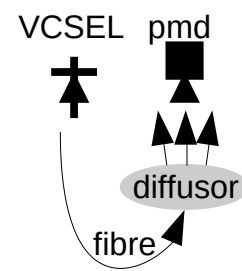


Figure 9: Diffusion layer between fibre end and detector

Variations or optimizations of this set-up need to consider the following issues:

- **Signal-to-Noise-Ratio (SNR):** each sampling point needs to be acquired with a reasonable SNR, i.e. with a reasonable modulation amplitude. Regarding the hardware set-up, this means that the signal attenuation over the fiber length is a key factor. Depending on the actual type of fiber used, the coupling of the VCSEL into the fibers can show a significant dependency of the resulting amplitude and the coupling angle so that the mechanical set-up needs to be sufficiently rigid.
- **Robustness:** in how far could vibrations or shocks result in tilts of the fibers and in how far does this influence the phase observed by the pmd?
- **The pattern does not need to fill the whole field of view.** In fact, with regard to the mutual dependency of the wiggling of the FPPN, it is advisable to find an optimum between the area covered by the pattern, which shall be minimized to avoid FPPN and lens distortion influences, the number of sampling points, which is supposed to be maximized so that the data fit for the wiggling function works best, and the damping in the fibers, which imposes restrictions on the feasible lengths and their orientation towards the camera.
- The optimization must keep in mind the targeted modulation frequencies, i.e. the unambiguous range must be covered to its full extent for the lowest frequencies used.
- Avoid multiple path propagation, ambient light influences and stray light¹.

pmd evaluated different types of fibers and found the following advantages and drawbacks (Table 3); for further reading, cf. [6].

¹ During operation, normally, ambient light does not affect the pmd camera operation, but for the calibration it is important to avoid even otherwise negligible sources of error.

Fiber Type	Short Description	Advantages	Disadvantages
Polymer Fiber	polymer core and cladding; cladding with lower index of refraction	<ul style="list-style-type: none"> • easy handling • cost effective 	<ul style="list-style-type: none"> • high damping • multi-mode propagation
Graded Index Glass Fiber	index of refraction attenuates smoothly from the core to the cladding	<ul style="list-style-type: none"> • low damping • broadly used, i.e. good availability 	<ul style="list-style-type: none"> • multi-mode propagation
Step-Index Glass Fiber	index of refraction attenuates stepwise from the core to the cladding	moderate damping	<ul style="list-style-type: none"> • multi-mode propagation
Single-Mode Glass Fiber	core and cladding have different indices of refraction	<ul style="list-style-type: none"> • extremely low damping • constant phase of the single mode 	<ul style="list-style-type: none"> • economically disadvantageous

Table 3: Fiber Types - Advantages and Drawbacks

For these reasons, the usage of graded index glass fibers is encouraged for the proposed kind of set-up.

In general, it is important that in general much care is taken for the fiber set-up. Keep the coupling from the VCSEL into the fiber bundle light-tight and keep the distance in between as short as possible (<5mm!!). The pmd sensor must not receive stray light not emerging from any fiber.

3. Software Set-Up / Algorithms

3.1. Intrinsic Lens Calibration

3.1.1. Calibration Model

The intrinsic lens calibration computes the relationship between arbitrary points in the Cartesian world coordinate system and their projection onto the 2D sensor coordinate system and vice versa. As projection model for the camera system, the pinhole camera model [3] is used² where all viewing rays from all pixels of the sensor meet in a common point. This common point is denoted as the “focal point” of the camera.

The projection vectors for pmd sensors which are derived by intrinsic lens calibration are computed from 9 parameters:

- **focal length:** (f_x, f_y) these values are commonly the same

² Any suitable lens calibration model may be used. If you have made good experiences with a different model, it may be used as well. It is only important to know that all subsequent calibration steps and the end-user application depend crucially on this lens calibration.

- **principal point:** (c_x, c_y) pixel-position of the principal point within the image
- **radial distortion:** (k_1, k_2, k_3)
- **tangential distortion:** (p_1, p_2)

The focal length describes the distance of the focal point from the image plane. The principal point is the position within the image plane where the viewing rays from the camera intersect orthogonally with the image plane. This is shown Figure 10.

In range imaging undistortion is usually applied in a different way compared to common 2D image undistortion. While the original 2D amplitude and distance image datasets are left

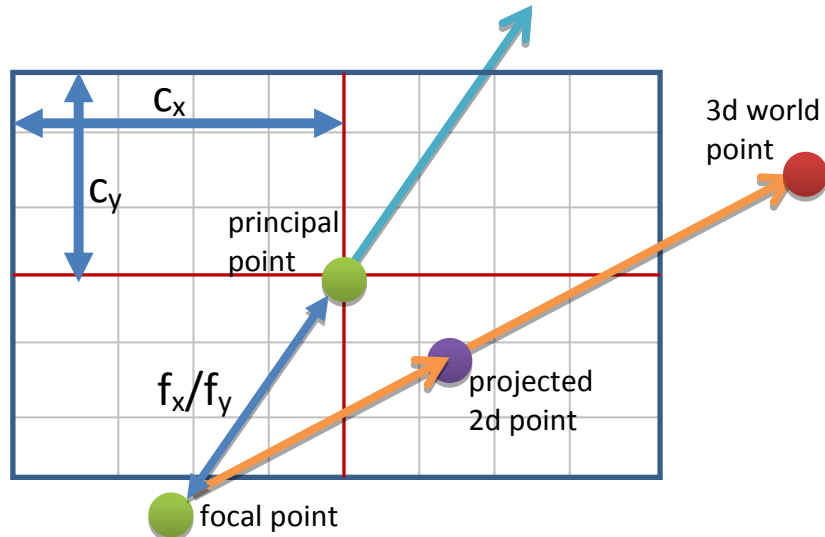


Figure 10: Intrinsic lens parameters without distortion

unchanged and no bilinear interpolation is done to compute rectified images, the unit vectors are aligned with the viewing rays and thus an undistorted 3D representation of the 2D data is computed. So, the 2D data of the sensor is left unchanged, distorted amplitude images remain distorted, but the 3D coordinates computed from these distorted 2D images deliver a 3D scene which will be undistorted (i.e. straight lines are straight again).

3.1.2. Feature Acquisition and Evaluation

For computation of the intrinsic parameters, feature constraints between feature points in 2D image space and the corresponding points in 3D world coordinates are needed. These constraint sets are commonly acquired using a planar checkerboard patterns which is imaged at a sufficiently large number of different world coordinate positions. This data is usually processed with OpenCV [5]. With regard to series production constraints, this approach is impractical. This is why the box calibration follows a different approach. As described in the section about the hardware setup, a pattern with feature points which are precisely known in the 3D world coordinate system is placed at only one position, i.e. neither the camera nor the pattern position is varied. Thus, no relative movement is required, a 'single shot' is sufficient.

As shown in Figure 11, the box's feature points are the middle points of circles which are detected with sub-pixel resolution by applying a threshold to the intensity image³. Prior to the point-wise detection, a predistorted template is correlated with the intensity image in order to be robust slight rotations or individual LED defects. For each point, a unit vector pointing into the direction of the corresponding viewing ray is computed: once based on the reference data and once based on the blobs identified during the image analysis. The essential part of the intrinsic lens calibration is now the estimation of the nine parameters mentioned above with the merit function being the minimization of the difference between both unit vectors. As the parameters are not linearly independent, a nonlinear optimization algorithm is required. **pmd's** internal empiric evaluations resulted in the application of a simple genetic algorithm.

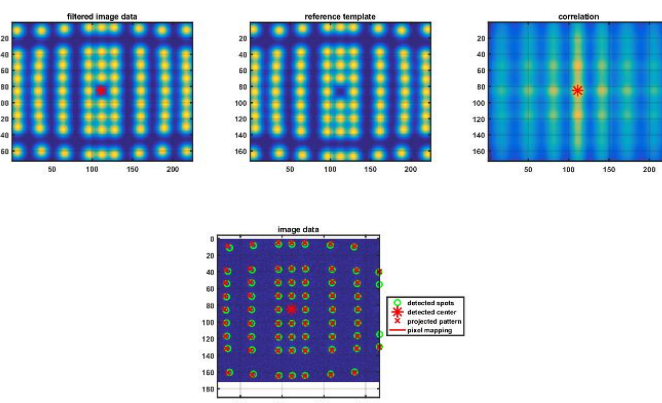


Figure 11: Feature point detection for the lens calibration

3.1.3. Quality Metric

When thinking about optimizations of the set-up or the algorithm with regard to the intrinsic lens calibration, it is necessary to have a metric defining the quality of the calibration. This is especially important in consideration of the fact that the parameter computation is non-linear.

An appropriate error measure can be obtained by reprojecting every feature point onto the image plane after the calibration. If the calibration was perfect, the projected 2D point would match the initially detected point. The actual shift for a feature point between its initially detected position and the reprojection from the corresponding 3D coordinate is called reprojection error. The error measure is then the mean reprojection error over all feature correspondences which were used to compute the intrinsic lens calibration parameters. According to our experience, acceptable reprojection errors are in the range of 0.1 to 0.5 pixels.

By the way, exactly this error measure is integrated into the algorithm to discard implausible or too bad results. The optimization is started again using different initial values for the genetic algorithm in this case. If the algorithm cannot derive parameters resulting an acceptable error message, the calibration is aborted and the calibration operator is asked to take appropriate actions. For instance, it might happen that dust or dirt causes pseudo features to be detected.

3.1.4. Global Lens Calibration

Depending on the actual lens being used, the manufacturing tolerances of the lens could be low enough to make a global calibration possible. This would be the case if the variability of the lens parameters determined for different lenses are in the same order as the typical variability of these parameters for one and the same module due to repetitions of the calibration process.

³ Intensity image with VCSEL shut off subtracted from intensity image with VCSEL being modulated

A partly global calibration can be applicable if the focal lengths and the radial and the tangential distortion parameters are stable while the principal points are not. This would mean that the calibration would only need to compensate the placing tolerances of the lens relative to the sensor middle point.

3.2. Wiggling

The so-called wiggling results in systematic distance deviations between the true and the calculated distance due to the fact that the underlying algorithm assumes ideally sinusoidal signals while the real signals comprise higher frequency fractions as well. This wiggling is a periodic function of the distance and oscillates with a wavelength that is one fourth of the unambiguous range. For details, confer [1].

While wiggling can be measured using a translation stage varying the true distance between the target and the camera, this procedure contradicts series production constraints. This is why the wiggling is measured by using a number of sampling points with different real phases as described in the section about the hardware set-up.

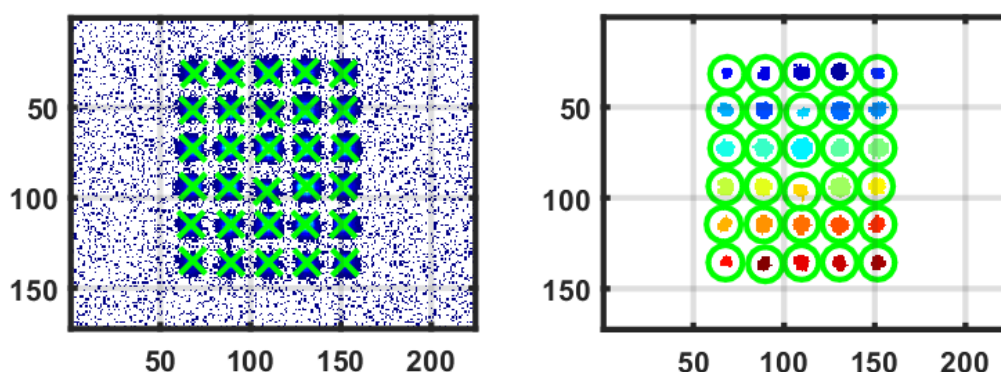


Figure 12: Fiber Segmentation (left: spot detection; right: ordered blobs)

To measure the wiggling effect and to compute the compensation factors, first, the intensity image⁴ is used for the initial segmentation to find the different fibers in the image (see Figure 12). Next, the individual blobs found during this segmentation need to be mapped to the appropriate fiber in order to ensure the correct mapping of real and measured phases. For this purpose, the regular geometrical arrangement of the fibers is exploited. As a result, for each fiber, the set of pixels representing it is known.

⁴ Intensity image with VCSEL shut off subtracted from intensity image with VCSEL being modulated

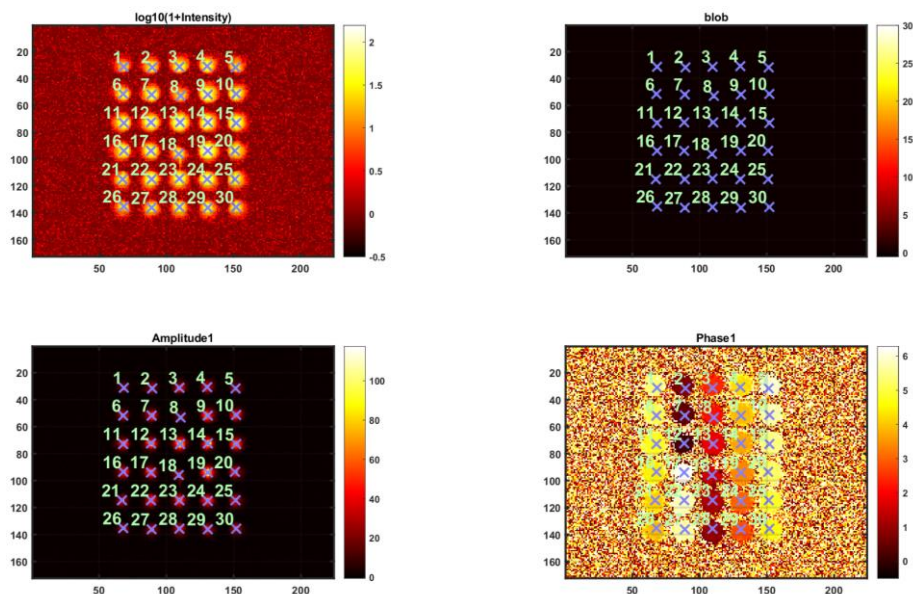


Figure 13: Fiber segmentation

The average values of the amplitudes and the phases of the pixel sets is computed after compensating the thermal drift effect and applying the initial FPPN estimation. In parallel to this computation, the fiber-to-camera distances, which are defined by the geometrical layout, are computed for each relevant pixel by considering the optical model. The deviation is the wiggling. The process needs to be performed for all modulation frequencies separately.

Due to the constraint that the sampling points need to cover the unambiguous range of the lower modulation frequency, the sampling points wrap around for the higher modulation frequency. Nevertheless, the implemented algorithm takes such values also into account; the wrapping is compensated by the modulus operation. In this way, they contribute to diminishing the influence of noise. Figure 14 shows the obtained wiggling for one camera module as an example.

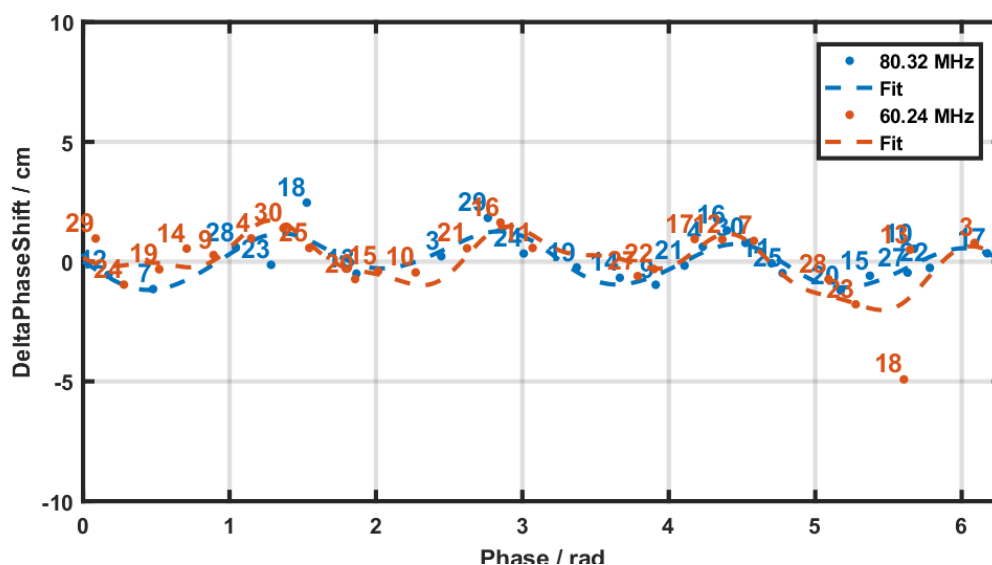


Figure 14: Phase Wiggling (the numbers denote the individual fibers)

The wiggling deviation can be modelled by the following equation:

$$\Delta_{wiggling}(\varphi) = x_1 \sin(\varphi + y_1) + x_2 \sin(2\varphi + y_2) + x_3 \sin(4\varphi + y_3) + x_4 \sin(8\varphi + y_4)$$

The software computes the fit parameters and stores them in the calibration file.

Not only is the phase falsified by the wiggling effect, but also the amplitude data. These compensation parameters can be derived from the same acquisition data.

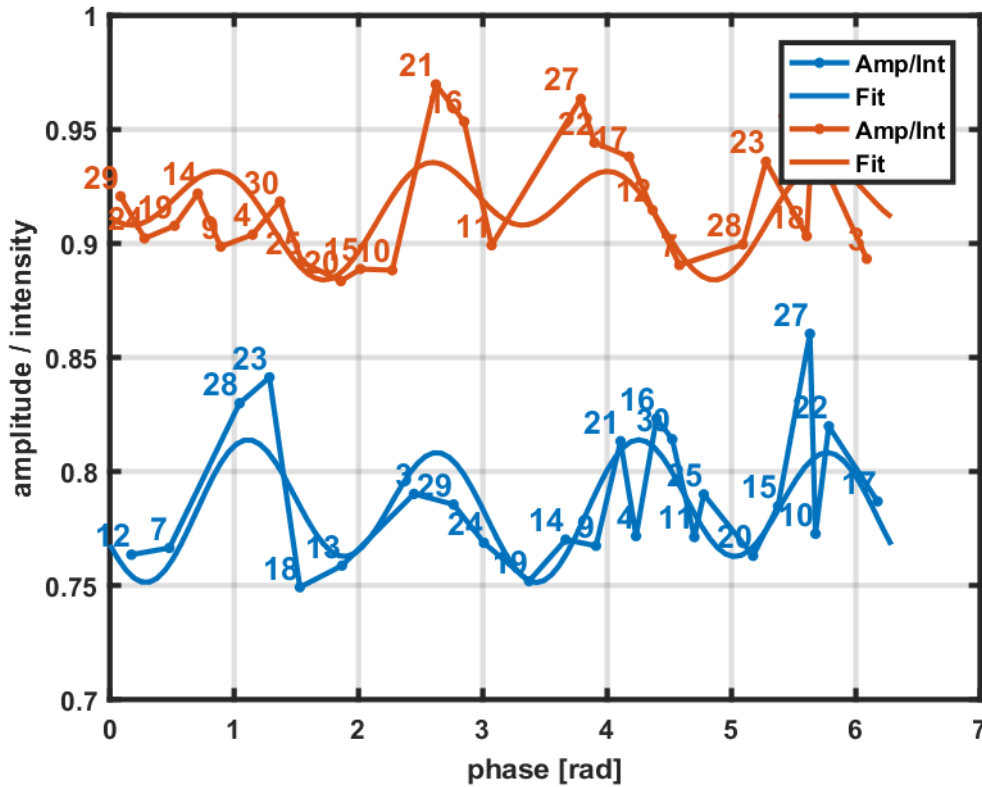


Figure 15: Amplitude Wiggling

The amplitude values for the pixels viewing the fibers is divided by the intensity data⁵ minus the mean dark intensity level. The result is called the scaled amplitude data. Following the same approach as for the phase wiggling, the wiggling parameters for the amplitude are determined by a non-linear optimization. The model for the wiggling resembles the phase model with an additional offset ϑ :

$$\Delta_{amplitude}(\varphi) = \vartheta + \sum_{i=0}^3 \alpha_i \sin(2^i \varphi + \gamma_i)$$

The merit function for the data fit is the sum of least squares to the raw data, see Figure 15.

⁵ The term 'intensity' refers to the uncorrelated part of the signal, i.e. the offset, while the term 'amplitude' describes the amplitude of the correlated part only. For a more detailed distinction, cf. [1].

3.2.1. Quality Metric

As the order of the wiggling error is in the range of approximately 10cm, the resulting fit can be checked quickly for plausibility by checking whether the amplitude of the wiggling function found as well as the maximum deviation between the fit and the raw data points are lower than this limit. Additionally, it should be checked whether the minimization algorithm converged to a solution at all. If these simple criteria are not satisfied, the sense of the wiggling calibration is reduced to absurdity and the calibration process should be aborted with an error.

3.3. Offset and FPPN Correction

Even having applied the wiggling and the temperature compensation, the resulting distance value shows a fixed offset towards the actual distance of the sensor to the object. In particular, this is due to individual sensitivities, offsets and signal propagation times of pixels. The offsets are characterized by a common mean value, which is simply referred to as 'offset', and a pixel-individual component. It can be seen analogously to the fixed pattern noise (FPN) of common 2D cameras. Consequently this difference is called fixed-pattern-phase-noise (FPPN).

For a pmd sensor system with a global offset o , a raw distance value d_i^r for pixel i and a fppn-value f_i for the same pixel, the offset-corrected distance d_i is computed as

$$d_i = d_i^r + o + f_i$$

Before o and f_i can be applied to the raw distance data their values must be computed. This is done by subtraction of ground truth distance values from measured values which have been acquired with the sample that is going to be calibrated. The ground truth distance value d_i^g for pixel i is obtained by placing the sensor in a known distance from a homogenously reflecting wall. Given the unit vectors (which are explained in the intrinsic calibration section), the distance d_o of the sensor to the wall and assuming the system is looking orthogonally at the surface, d_i^g can be computed as

$$d_i^g = \sqrt{(d_o * v_i^x)^2 + (d_o * v_i^y)^2 + (d_o * v_i^z)^2}$$

The pixel-individual offset o_i (which incorporates the global offset o) is computed as the difference between the measured raw distance d_i^r and the ground truth d_i^g and is equal to the sum of the offset and the FPPN of the pixel

$$o_i = d_i^r - d_i^g = o + f_i$$

With o being the mean value of all pixel-individual offsets o_i

$$o = \frac{1}{n} \sum_{i=1}^n o_i$$

The FPPN f_i for pixel i is computed as

$$f_i = o_i - o$$

The data sequence which is used for getting the d_i^r values should be recorded with a reasonable integration time and averaged over a sufficient number of frames in order to minimize the temporal noise of the system such that the offset data becomes most reliable. According to our experience, using 10 frames with an integration time of 1µs is acceptable.

3.4. Mutual Dependency of Wiggling and FPPN

The most important pitfall to keep in mind is the mutual dependency of the fixed phase pattern noise and the wiggling. The distance data, which is acquired for the determination of the pixel-individual offsets, is falsified by the wiggling effect, which is unknown at this stage. Likewise, the wiggling effect cannot be measured without knowing the FPPN. A prerequisite for calibrating both effects is the knowledge of the optical model.

This mutual dependency can be decomposed with a different hardware set-up. An accurate normal movement between the camera module and the target results in a measurement including both the FPPN and the wiggling effect. The optical model will not be required for the computation of the wiggling correction parameters if only the pixels are used which are normal to the reference, i.e. the orientation of the camera does not matter, too. Likewise, the pixel offsets are not required because one can evaluate only the relative position changes. Subsequently, the FPPN can be computed with wiggling-free data.

Typically, however, such a set-up causes too much effort and consumes too much time for a series production. This is why a different approach is used. For the FPPN, an initial estimate is made by simply subtracting the optical pathways from the FPPN measurement. Using this estimate, the wiggling is computed. Afterwards, the data acquired for the FPPN calibration is compensated regarding the wiggling.

3.5. Temperature Drift

Due to the fact that the internal capacitance of the illumination depends slightly on its temperature, there is a temperature dependent shift of the signal phase resulting in a global distance offset of the complete image. The distance drift can be caused by an ambient temperature change or by the current induced temperature rise inside the illumination. Regardless of the cause, since the distance drift scales with the temperature over the relevant temperature range, this drift is corrected using a temperature sensor positioned close to the illumination. Figure 16 shows the raw data of the distance deviation caused by temperature drift and an appropriate fit for 80 and 60MHz. The start and the end temperature is based on the self-heating effect during a typical application acquiring 100 frames at an integration time of 5ms.

Please note that after changes that affect the current induced heating, i.e. a change of the integration time or the frame rate, small drifts might still occur within short timeframes of a few seconds, since the measured temperature lags behind the current illumination temperature.

The temperature analysis is usually done for a series, or charge, of cameras. Typically, the coefficients for different cameras are quite similar (difference smaller than 10%). Thus the resulting correction coefficients can be averaged to yield a global correction value for all cameras. This can be proven by the analysis of the calibration data of a statistically relevant number of pmd modules. FF shows the result, i.e. the variation of the slope of the thermal drift regression. 90% of the modules show a slope within a range of 1.17 to 1.34mm per degree Celsius. If the global slope value of 1.25mm per degree Celsius was used for all cameras was,

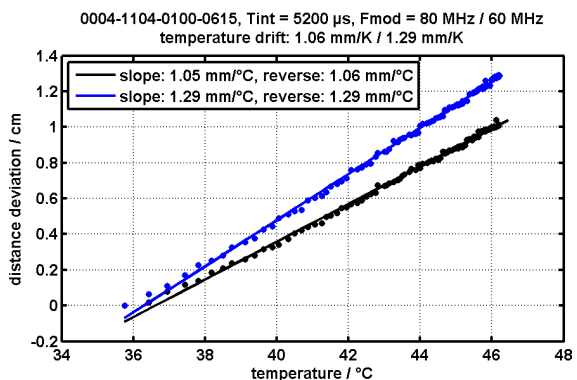


Figure 16: Distance deviation caused by thermal drift – linear relationship

the distance deviation for the module with the actual calibration value of 1.17 would amount to less than 2mm for a temperature difference of 20 degrees. On the other hand, the application of a global thermal drift calibration saves about 10min per module.

Consequently, the best practice for the calibration of the thermal drift respecting series production

constraints is to determine the thermal drift globally by the procedure described in [1] and to repeat the procedure in case of changes of assembly parts / electronic devices.

Alternatively, the thermal drift can be determined for each camera module by using the calibration box suggested for the FPN determination according to [1]. However, that would imply an additional timing demand of several minutes.

3.6. Illumination Mask

For the case that the field which is illuminated by the VCSEL does not cover the whole field of view of the sensor (which can happen if this is designed on purpose), the calibration can determine the useable region of interest. This process is called the determination of the illumination mask. This mask can be determined quite simply using the set-up proposed for the first calibration box (a homogeneously illuminated target), as those pixels which do not yield any modulation data at all should be masked. Such a case is shown in Figure 18. Please note that that such an illumination mask is likely not to be applicable at all, because usually the VCSEL is designed to fit to the sensor and lens.

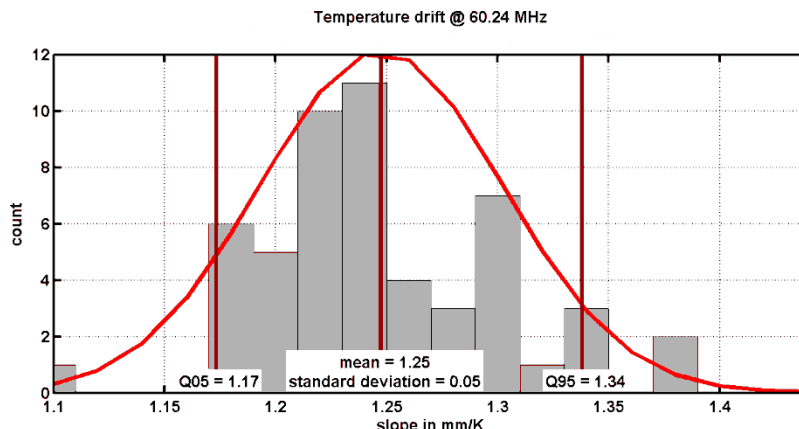


Figure 17: Temperature drift

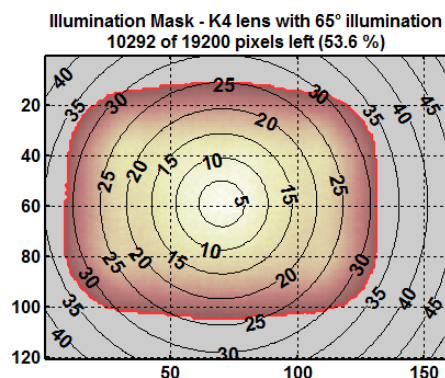


Figure 18: Illumination Mask Example

4. Data processing

This section describes how the calibration parameters are used during normal operation. This is useful as further background information for the actual calibration.

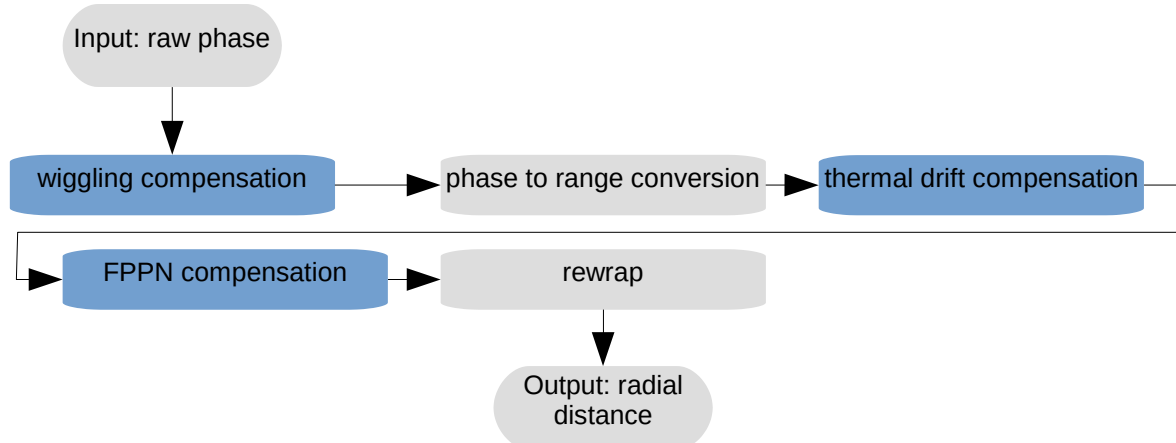


Figure 19: Data Processing Part 1/2 (blue parts require calibration inputs)

Having acquired the raw data for each modulation frequency involved, the first step is to apply the amplitude and phase wiggling compensation as shown in Figure 19. As all further calibration steps are not applied to the phase measured in degrees, the next step is to convert the phase to distance data. Then the thermal drift is compensated.

As one of the last steps, the fixed phase pattern noise offsets are applied. Then the distance values need to be rewrapped according to the unambiguous range because the previous calibration steps might have resulted in a violation of this limit.

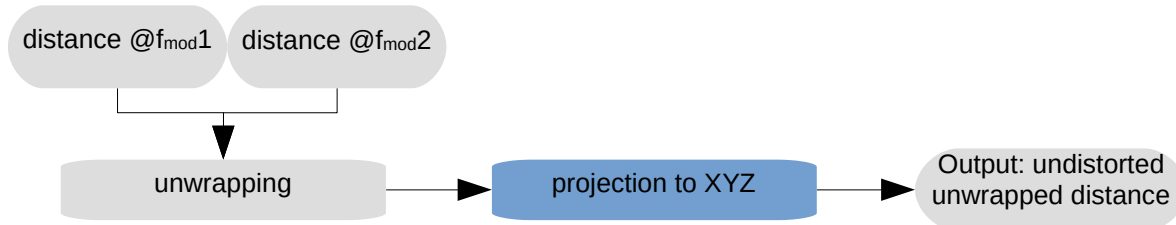


Figure 20: Data Processing Part 2/2 (blue parts require calibration inputs)

Now the distance data is known individually for each modulation frequency. For any pixel, each distance is presumably wrong because of phase wrapping, so that the total unambiguous range is shifted to the least common multiple of the individual ranges by subsuming the individual distances. Finally, Figure 20 shows that the radial distance found in the former step is projected into the Cartesian XYZ world coordinate system by means of the intrinsic lens parameters.

The compensation of the amplitude wiggling effect is required to have comparable, scaled amplitude data. This is used to predict the distance noise and the flag probably implausible distance values.

In parallel to the compensation of the distance- and amplitude-related effects, the fixed pattern noise of the intensity image (if available) can be compensated.

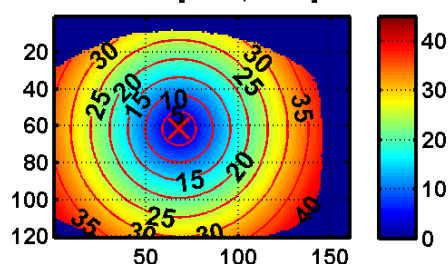
5. Calibration Results

The series production determination of the calibration parameters is carried out with limitations regarding the set-up. These limitations are supposed to deteriorate the results. This is the reason for a comparison of the results with those obtained for a prototype calibration (section 5.1). Afterwards, both results are compared using a specific error metric (section 5.2).

5.1. Comparison of the Individual Steps

The optical model delivers the principal points and the distortion parameters. An intuitive way to compare the results obtained by different calibration methods is to visually oppose the inclination angles over the whole field of view. See Figure 21 for an example for the same camera module, which was calibrated once using the prototype and then with the series calibration. One can see that the center point is slightly displaced while the inclination angles are comparable. In this example, the center point dislocation is due to a slight imprecision of the mechanical set-up which could be resolved subsequently. However, this shows that the calibration targets and housings need to be designed and handled very carefully.

Inclination angles in deg of OpenCV92 calibration
center = [67.92, 61.31]



Inclination angles in deg of Box92_2 calibration
center = [68.92, 65.02]

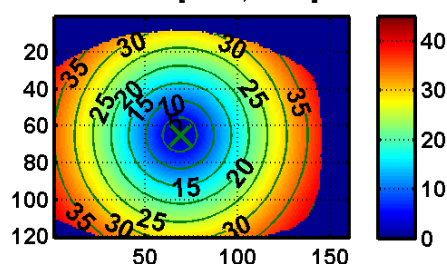


Figure 21: Opposed Calibration Inclination Angles

With regard to the wiggling effect, the amplitude and the shape of the wiggling compensation is interesting. This is shown in Figure 22. One can see deviations in the order of 15mm. Obviously, the deviation increases over the distance. This is caused by the low signal quality of the fibers at the end of the unambiguous range.

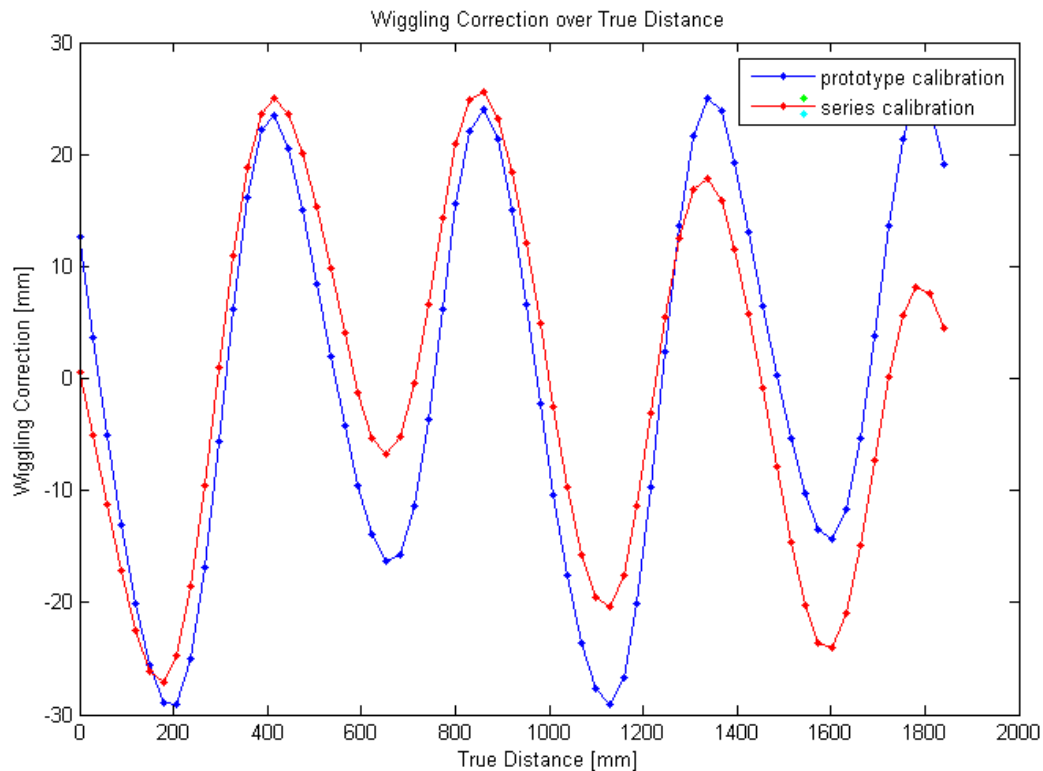


Figure 22: Phase Wiggling Compensation with prototype and series calibration

FPPN can be compared best when selecting one pixel row because this pixel row crosses the three modulation areas of the chip so that all relevant effects are comprised in such a single line. This is shown in Figure 23. The term 'initial' refers to the initial estimation of the FPPN on the distance falsified by the wiggling effect. This effect is supposed to be compensated in the last data row ('final').

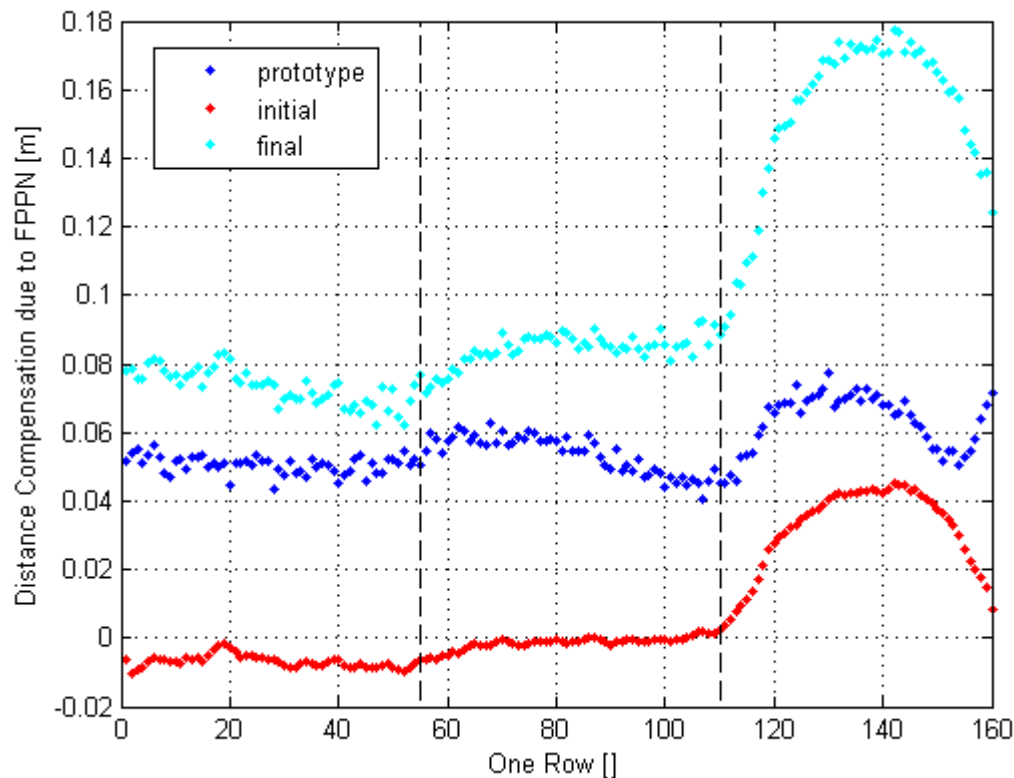


Figure 23: One Row of the FPPN

5.2. Metric-Based Comparison

The last section revealed non-negligible differences regarding the individual calibration steps of both concepts. However, the question is to which extent these differences result in actual distance differences. This question can be answered by comparing the difference of a new⁶ measurement with ground-truth data using both calibration sets individually for the same camera module.

Such a plot is given by Figure 24 for one arbitrary reference pixel. One can see that the distance differences show the same order both for the mean value and also for their standard deviation.

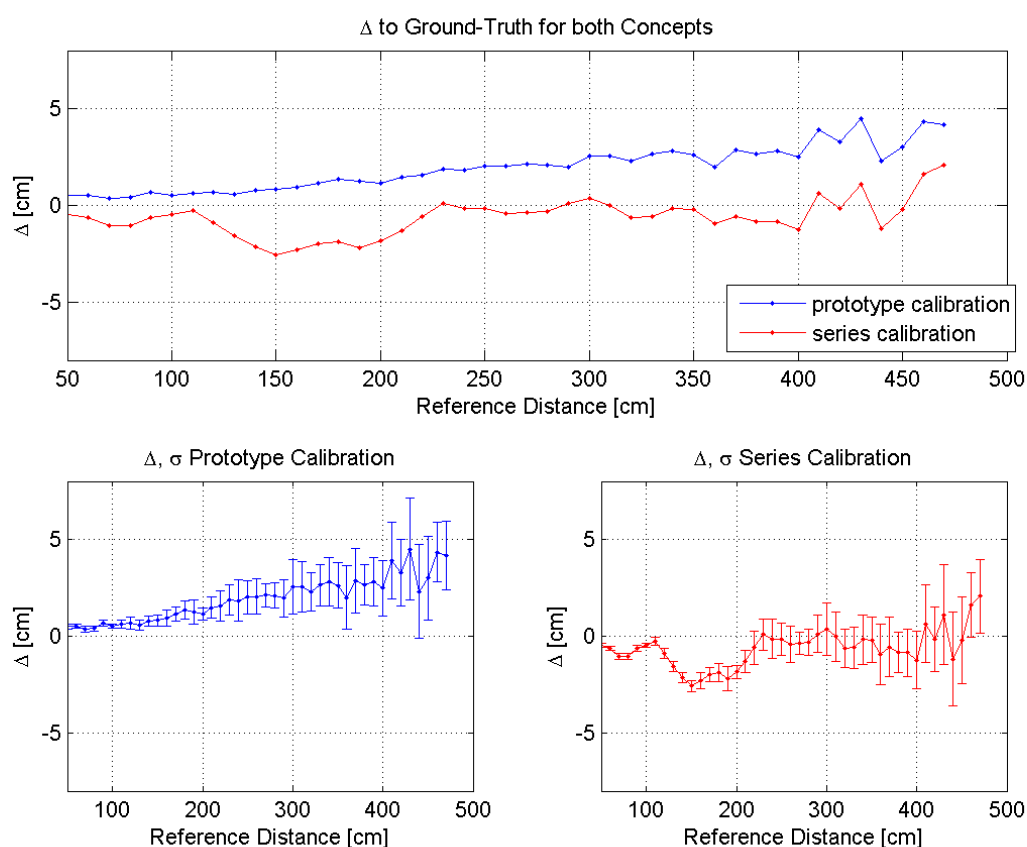


Figure 24: Difference to Ground-Truth with Applied Calibration; reference pixel in the middle

⁶ In this context, 'new' means 'not used for the calibration itself'. Yet, the same camera module is used as for the calibration.

6. Parameters

Table 4 lists the parameters which either need to be supplied by the designer of the calibration boxes because they are hardware-dependent or which can be used for optimization purposes.

Calibration Section	Parameter	Unit	Description
Optical Model	Inner Radius	[pixel]	Approximate inner radius of the circular points
	Outer Radius	[pixel]	Approximate outer radius of the circular points
FPPN	targetdistance	[m]	Orthogonal component of the distance between the target and the camera
Wiggling	laserToFiberDist	[m]	Coupling distance d_c - cf.
	Threshold_fiber_min_amp	[digits]	Used for the segmentation: discard pixels with lower / higher amplitudes
	Threshold_fiber_max_amp		
Global	ROI	[pixel]	Initial ROI for the acquisition of the calibration images.

Table 4: Set-up Parameters

Apart from the parameters listed here, there are some common basic parameters as for example the integration time, the frame rate, the duty cycle or the modulation frequency to be used for the individual acquisitions. Furthermore, the number of frames used for averaging (and thus noise-reduction) purposes can be specified.

References

- [1] **pmdtechnologies ag**: Application Note 1, 2014
- [2] **pmdtechnologies ag**: Calibration Concept Video, 2014
- [3] http://en.wikipedia.org/wiki/Pinhole_camera_model (last visit Oct. 30th, 2014, rev. 630830640)
- [4] Süße, Rodner: "Bildverarbeitung und Objekterkennung", ISBN 978-3-8348-2605-3, DOI 10.1007/978-3-8348-2606-0, Springer Verlag 2014
- [5] OpenCV web site: <http://opencv.org/about.html> (last visit Nov. 10th, 2014)
- [6] Ziemann et al.: „POF-Handbuch - Optische Kurzstreckenübertragungssysteme“, ISBN 978-3-540-49094-4, DOI 10.1007/978-3-540-49094-4, Springer Verlag 2007

Document History

Document title: Series calibration – Cal-12-1-AN

Revision	Origin of Change	Submission Date	Description of Change
0	OLo	2016-02-18	New Application Note
1	OLo	2016-05-12	Updated and added some images and photos

© **pmd**technologies ag, 2016

Mailing Address: **pmd**technologies, Am Eichenhang 50, 57076 Siegen, Germany

Technical information subject to change without notice.

This document may also be changed without notice.

All texts, pictures and other contents published in this application note are subject to the copyright of **pmd**, Siegen unless otherwise noticed. No part of this publication may be reproduced or transmitted in any form or by any means, electronic or mechanical, including photocopy, recording, or any information storage and retrieval system, without permission in writing from the publisher **pmd**.